

Spin casting characterization: An experimental approach for the definition of runners design guidelines

*Original*

Spin casting characterization: An experimental approach for the definition of runners design guidelines / Vezzetti, Enrico.  
- In: JOURNAL OF MATERIALS PROCESSING TECHNOLOGY. - ISSN 0924-0136. - 196:1-3(2008), pp. 33-41.  
[10.1016/j.jmatprotec.2007.04.134]

*Availability:*

This version is available at: 11583/1835360 since:

*Publisher:*

ELSEVIER SCIENCE

*Published*

DOI:10.1016/j.jmatprotec.2007.04.134

*Terms of use:*

This article is made available under terms and conditions as specified in the corresponding bibliographic description in the repository

*Publisher copyright*

(Article begins on next page)

**NOTICE:** this is the author's version of a work that was accepted for publication in "Journal of Materials Processing Technology". Changes resulting from the publishing process, such as peer review, editing, corrections, structural formatting, and other quality control mechanisms may not be reflected in this document. Changes may have been made to this work since it was submitted for publication. A definitive version was subsequently published in Journal of Materials Processing Technology, Volume 196, Issues 1–3, 21 January 2008, Pages 33–41  
DOI:10.1016/j.jmatprotec.2007.04.134

## SPIN CASTING CHARACTERIZATION: AN EXPERIMENTAL APPROACH FOR THE DEFINITION OF RUNNERS DESIGN GUIDELINES

E. Vezzetti

*Dipartimento di Sistemi di Produzione Ed Economia dell'Azienda, Politecnico di Torino, Corso Duca degli Abruzzi 24, 10129, Torino, Italy, Ph: +39 011 5647294 Fax +39 0115647299*  
[enrico.vezzetti@polito.it](mailto:enrico.vezzetti@polito.it)

The present attention to production cost and time reduction has encouraged many factories to employ some non conventional technologies instead of the conventional ones for mould production.

These specific non conventional manufacturing technologies, aimed at achieving a significant time reduction for tools manufacturing, are commonly called rapid tooling techniques.

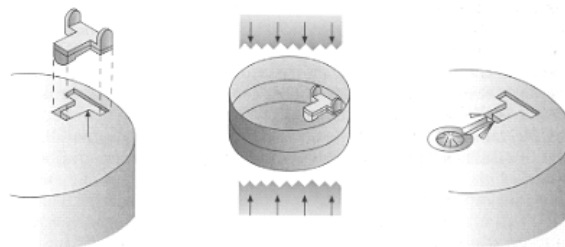
Among these rapid tooling methodologies, it is possible to find one of the most direct and flexible techniques which enables, by using a non-cured silicone, the manual shaping of a physical object obtaining directly the mould after some additional handmade refinements.

In order to know how the process parameters influence the final shape of the cast object, this work develops an experimental analysis for the estimation of a preliminary model for the process characterization.

**Keywords:** Rapid Prototyping, Rapid Tooling, Spin Casting.

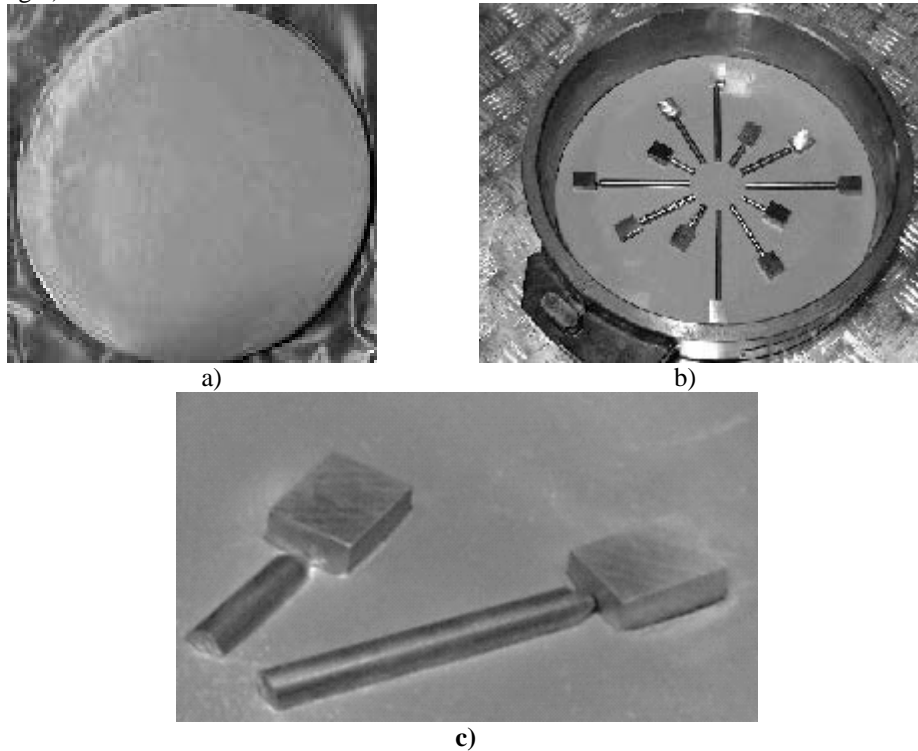
### 1. Introduction

The mould manufacturing represents one of the most expensive phases of the entire product development cycle. For this reason, the great competitiveness that characterizes the actual manufacturing market has obliged most manufacturers to increase their attention on time and cost saving technologies, especially for the realization of low volume productions. As a result of this innovation process, a lot of factories have introduced, inside their design and manufacturing phases, the use of rapid technologies. The use of these techniques in the design and manufacturing of production tools (e.g., moulds) has given a great advantage mainly in the manufacturing of complex geometries. These specific techniques, better known with the name of **rapid tooling**, could be employed for the realization of pre-series moulds working directly with a layer by layer technique (*direct tooling*), or for the realization of tool masters (*indirect tooling*) [1]. All these applications are characterized by a high flexibility level in terms of reachable complex geometries and by a significant reduction of tool manufacturing time. One of the most interesting indirect rapid tooling techniques, especially in terms of equipment and employed material cost, is "**spin casting**". This methodology is very simple and characterized by the presence of two fundamental elements: silicone rubber and centrifugal force (see Fig.1).



**Figure 1:** Spin Casting Mould

The presence of uncured silicone rubber, resistant to temperatures around 550°C and featuring plastic behaviour at the beginning of the process, permits a significant flexibility to the process for the manufacturing of very complex geometries (see Fig.2).



**Figure 2:** a) Uncured silicone rubber disk. b) Master imprint. c) A particular of master imprint.

## 2. Spin Casting

The spin casting process starts with the master models (often created with rapid prototyping systems), cores, pull-out sections and locating pins laid out on the disc of uncured silicone rubber. After this step, the two discs are mounted into a vulcanising frame where the combination of heat and pressure forces the silicone into all crevices, around all details, and cures the silicone.

The resulting mould is tough, resilient, dimensionally accurate, heat and chemically resistant. After vulcanisation, the mould is easily fixed to release the patterns (and later, parts) from the cavities. This is true even for patterns with a wide variety of undercuts. In order to complete the realization of the mould, gates, runner system and air vents are cut into the cured rubber mould with a sharp knife or scalpel. Air vents may also be drilled into the cavity to aid in-venting of entrapped air or gas.

After these steps, the two silicone disks are ready to be located on the spin caster machine, where they are pressed by means of two disks, in order to avoid molten material escape during the rotation. This mould can be employed for the definitive casting process for a number of times principally related to the alloy type and dimension of the disk cavities, which have been generated by the master accommodation in the uncured silicone disk. Both these variables are strictly related to the casting process parameters: casting temperature  $T_c$ , disk closing pressure  $p$ , casting time  $t$  and rotational speed  $\omega$  [2,3].

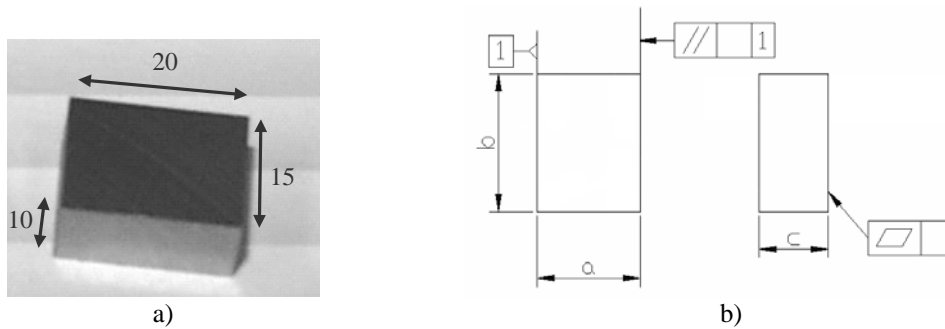
In order to improve the quality of the cast products, the behaviour of process parameters has been studied. Some research activities have been developed on the cooling process, highlighting the necessity to extend the mould life, which is limited by the thermal stress involved in the process, and to reduce the production cycle [4]. The importance of the spin-casting cooling process and its correlation with the different cast geometries and their quality has driven to the development of a numerical simulation method [5]. This study has also shown that some factors, such as the clamping time, intensity of convection heat transfer, the use of a mould processing-table with a metal surface are important factors affecting the cooling process and the solidification time. As a consequence of the results obtained in the first experimentation, that show the correlation of the cast product quality with the thermal conditions, an air based cooling system has been designed and studied in order to understand how it could improve the thermal behaviour of the mould [6].

Moreover, also the mould design and mainly the runners influence the efficiency of the casting process. As described before, at present this process is often manual and iteratively repeated until a good solution is reached [7].

Starting from these evidences, this paper presents a structured experimental analysis of the spin casting process that permits to define some preliminary guidelines for process design aimed at reducing the presence of anomalies in the cast objects. The attention is focused on runner design.

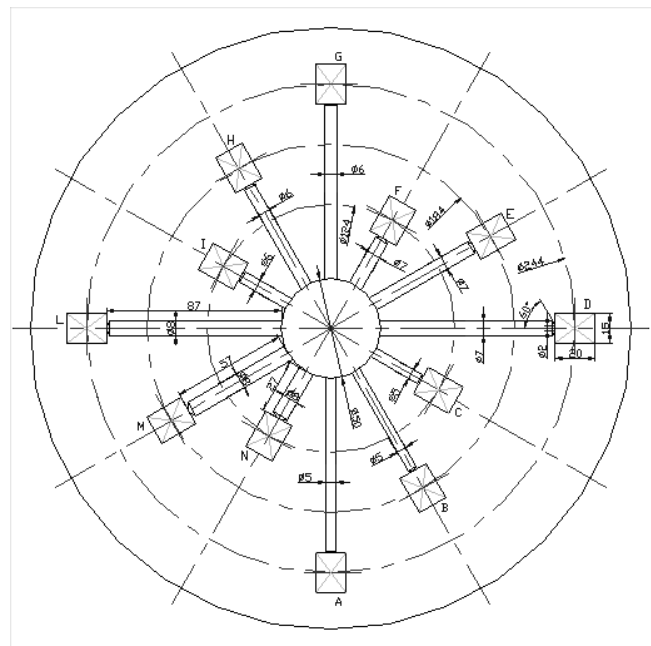
### 3. Experimental work

Starting from the considerations mentioned before, an experimental analysis of the casting process parameters and runner typologies has been performed. In order to obtain more accurate information about the influence of the different parameters, the rapid prototyped masters have been substituted by steel made ones. Working with simple steel made geometries (parallelepipeds) it is simpler to obtain reliable information about the dimensional and geometrical tolerances (*parallelism* and *planarity*) provided by the casting process. On the other hand, the use of steel made masters is also related with the necessity to assure that, during the vulcanising process, the masters maintain the original shape even under the application of pressure. The dimensional and geometrical tolerances of the parallelepipeds have been measured by a Coordinate Measure Machine (CMM) (see Fig.3).



**Figure 3:** a) Parallelepiped benchmark. b) Analyzed dimensional and geometrical tolerances.

After the choice of the tool masters, the attention has been moved to the runner design [8]. Commonly, two different manufacturing strategies can be chosen for their design. It is in fact possible to work with a direct runner, which normally takes the molten material from the disk centre directly to the imprints, or with an indirect one, which employs an intermediate grit and a secondary smaller runner stemming from it in order to access the master imprints. Moreover, a second variable in the runner design is related to the access to figure imprints: it can be *top* if the access is from the figure centre or *low* if it is from the opposite side. In order to have a more strict control on the dimension of the runners, therefore reducing the influence of other geometrical issues caused by the presence of the intermediate grit and more complex runner shapes, the experimental phase has been performed employing a **direct top** configuration (see Fig.4).



**Figure 4:** Runner configuration.

In order to develop a more consistent analysis, the runners have been obtained during the mould preparation, imprinting them by using steel cylinders at the same time of the other masters on the uncured silicone rubber disk. In order to evaluate the influence of the figure imprint distance from the centre and the runner diameter, a set of cylinders with different lengths and diameters has been selected (see Fig.5).



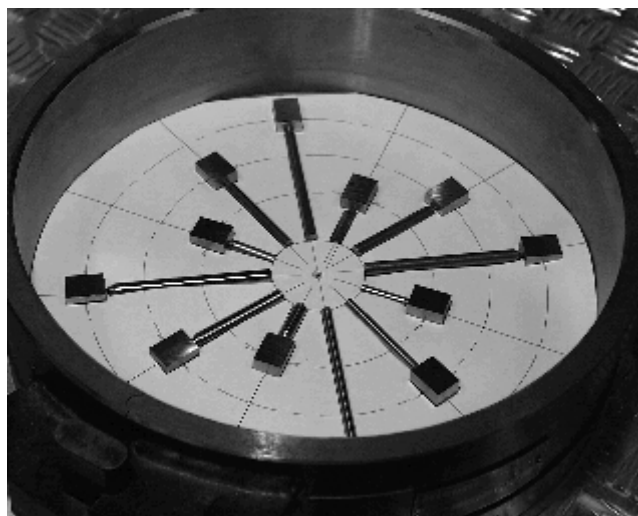
**Figure 5:** Steel cylinders employed for runners imprinting.

In order to complete the experimental set, twelve different runners have been chosen with four different diameter values and three different lengths (see Tab.1).

**Table 1:** Dimensions of the cylinders employed for the realization of runners.

Cylinder number	Length [mm]	Diameter [mm]
1	27	5
2	57	6
3	87	7
4	27	8
5	57	5
6	87	6
7	27	7
8	57	8
9	87	5
10	27	6
11	57	7
12	87	8

Moreover, in order to guarantee the balancing of the molten material during the casting process on the whole mould figure, the tool masters have been located on the disk with a central symmetrical configuration (see Fig.6)



**Figure 6:** Runners and masters location design

For this experiment, the use of a unique silicone rubber and alloy has been assumed in order to focus the attention on the process parameters and runners dimensions. The chosen silicone rubber was a **BV65HVLD30010** rubber (see

Tab.2), one of the hardest actually available. This rubber guarantees the highest possible number of cast parts. The employed casting alloy was a Zinc based alloy called ZAMA. It has been chosen for its low melting properties, reduced cost and good surface roughness (see Tab.3).

**Table 2:** Silicone rubber properties.

Name	Disk Diameter [mm]	Disk Thickness [mm]	Hardness [Shore A]
<b>BV65HVLD30010</b>	300	10	65

**Table 3:** Zinc alloy properties.

Name	Density [Kg/dm <sup>3</sup> ]	Specific Heat [J/kg K]	Optimal Casting Range [°C]	Thermal conductivity [W/m K]
ZAMA	6.92	382	420-460	113

Starting from the technical information about rubber and alloy given by the producer, the set of experiments [9] (see Tab.4) has been carried out with a range of angular speeds between 500 rpm and 600 rpm and pressure values from 2 bar to 3 bar. In order to verify whether the variable range has been correctly chosen, two tests on the range limits have been run. With 400 rpm the mould was not completely filled, while at 800 rpm and 3 bar pressure the molten material flowed out of the mould without completely filling all the figures (see Fig.7)



**Figure 7:** Non controlled material escape and incomplete figure filling.

**Table 4:** Scheme of the performed experimental tests .

N° Test	$\omega$ [rpm]	p [bar]	t [min]	Tf [°C]
1-2	500	2.5	1' 20''	450
3-4	500	3	1' 20''	450
5-6	500	2	1' 20''	450
7-8	550	2	1' 20''	450
9-10	550	2.5	1' 20''	450
11-12	550	3	1' 20''	450
13-14	600	2	1' 20''	450
15-16	600	2.5	1' 20''	450
18-19	600	3	1' 20''	450
20	700	3	1' 20''	450
21	400	3	1' 20''	450
22	800	3	1' 20''	450

In order to permit a successive consistent comparison between the cast parts, a disk integrity evaluation has been performed after every casting step. In particular, it has been checked the presence of scorches on the subdivision plane between the two disks, of micro bubbles on the figure surface, of little crevices in the figures, and silicone abrasion

inside the master figures, that could modify significantly the results of the successive casting steps. While all the tests were repeated twice, tests 21, 22 and 23 were run once because they employed limit conditions.

#### 4. Results Analysis

After the development of the entire experimental set, the dimensional information have been gathered with the use of a Coordinate Measure Machine (CMM) working firstly on the vulcanized silicone rubber before casting, in order to evaluate the actual linear shrinkage of the silicone rubber. Comparing the values (see Tab.5 and Tab.6) on the rubber disk with those on the steel masters, the average measured linear shrinkage results less than 1%.

**Table 5:** Dimensions of the steel masters employed for the mould preparation.

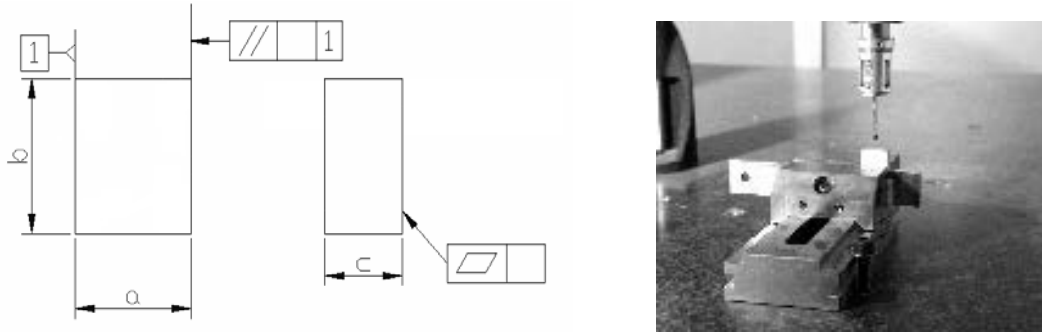
	<b>a</b> [mm]	<b>b</b> [mm]	<b>c</b> [mm]
<b>A</b>	14.99	19.96	9.99
<b>B</b>	14.98	19.97	9.99
<b>C</b>	14.99	19.98	9.99
<b>D</b>	14.99	19.96	10.00
<b>E</b>	14.99	19.98	9.99
<b>F</b>	14.99	19.95	9.99
<b>G</b>	15.01	19.97	9.97
<b>H</b>	15.00	19.97	9.98
<b>I</b>	14.99	19.97	9.98
<b>L</b>	14.99	19.97	9.97
<b>M</b>	14.99	19.96	9.98
<b>N</b>	14.99	19.96	10.00

**Table 6:** Dimensions of the master imprints after the vulcanising process.

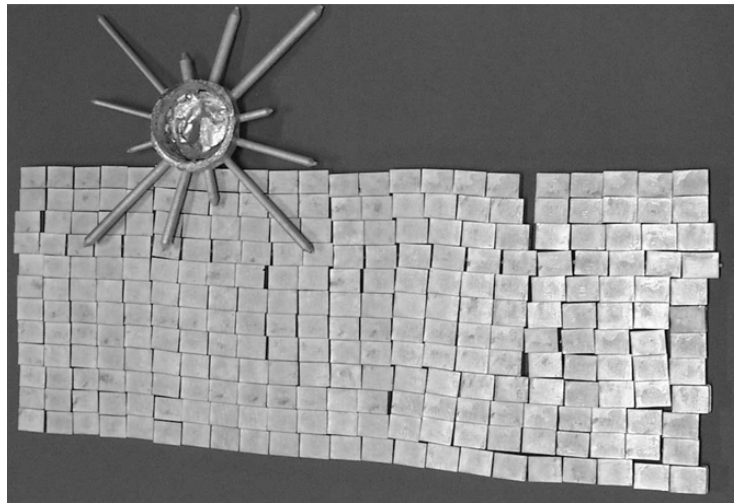
	<b>a</b> [mm]	<b>b</b> [mm]
<b>A</b>	14.99	19.74
<b>B</b>	15.02	19.85
<b>C</b>	15.00	19.77
<b>D</b>	14.99	19.78
<b>E</b>	14.91	19.75
<b>F</b>	14.96	19.75
<b>G</b>	14.92	19.81
<b>H</b>	15.03	19.79
<b>I</b>	15.02	19.92
<b>L</b>	14.98	19.90
<b>M</b>	15.07	19.82
<b>N</b>	15.07	19.88

After the preliminary measuring of the silicone disk, all the cast figures have been measured analyzing, for each of them, dimensions (a, b, c) and evaluating the geometric tolerances in terms of parallelism and planarity (see Fig.8 and Fig.9).





**Figure 8:** Geometrical and dimensional parameters evaluated on the cast objects with the use of CMM.



**Figure 9:** Cast elements obtained with the experimental set.

By means of a standard deviation analysis [10] and a polynomial regression [11], the experimental results have been analyzed in order to derive the process parameters, the runner dimensions and the cast objects relations.

$$y = k + x_1 \cdot \omega + x_2 \cdot p + x_3 \cdot d + x_4 \cdot D + x_5 \cdot \omega^2 + x_6 \cdot p^2 + x_7 \cdot d^2 + x_8 \cdot D^2 + x_9 \cdot \omega \cdot p + x_{10} \cdot \omega \cdot d + x_{11} \cdot \omega \cdot D + x_{12} \cdot p \cdot d + x_{13} \cdot p \cdot D + x_{14} \cdot d \cdot D$$

where

$k, x_i, i = 1, \dots, 14$	Coefficients of the polynomial function
$y$	Dimension of the parallelepiped
$w, p, d, D$	Independent variables (process parameters)

Starting from the results obtained from the experimental tests, a regressive polynomial function has been obtained for dimensions  $a, b$  and  $c$  of the parallelepiped. The obtained functions result in different reliability values (see Tab.7).

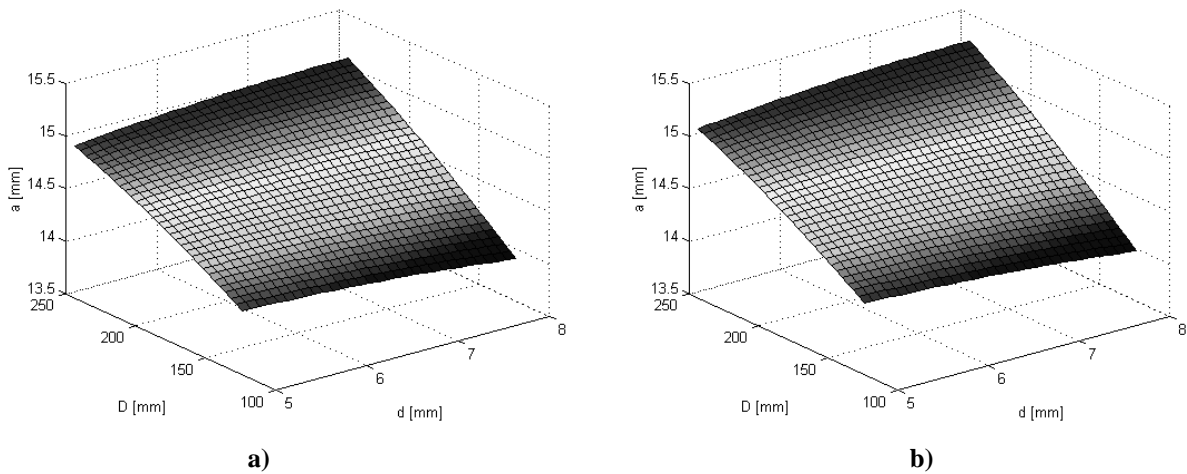
**Table 7:** Reliability values obtained for the different parallelepiped dimensions.

Dimension	$R^2$
$a$	0.963
$b$	0.621
$c$	0.742

Therefore, in order to show only the most significant information, also due to the reduced available space, only the data for dimension  $a$  are shown, considering also that its polynomial reliability is the highest one and nearby one.

$$y = 12.12 + 0.970 \cdot p - 0.225 \cdot p^2 - 0.0142 \cdot d^2 - 0.0000144 \cdot D^2 + 0.0000152 \cdot \omega \cdot D + 0.000937 \cdot d \cdot D.$$

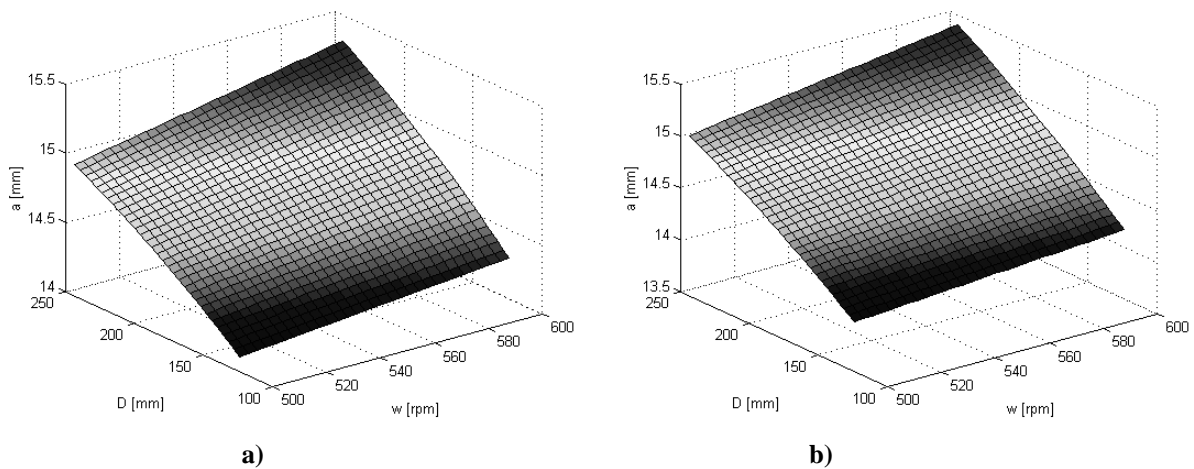
Working with the polynomial regression, some specific considerations have been derived by graphically analyzing dimension  $a$  and fixing two variables in each graph. From the first analysis, the function behaviour (see Fig.10) shows that, moving the master imprint far from the centre of the disk, therefore increasing the value of variable  $D$  (the runner length), the dimension of the cast parallelepiped increases. For variable  $d$  (the runner section diameter), if the master imprint is located near the centre, the dimension of the cast parallelepiped seems to be indirectly proportional to the section variation.



**Figure 10:** a)  $\omega = 500$  rpm and  $p = 2$  bar b)  $\omega = 550$  rpm and  $p = 2.5$  bar

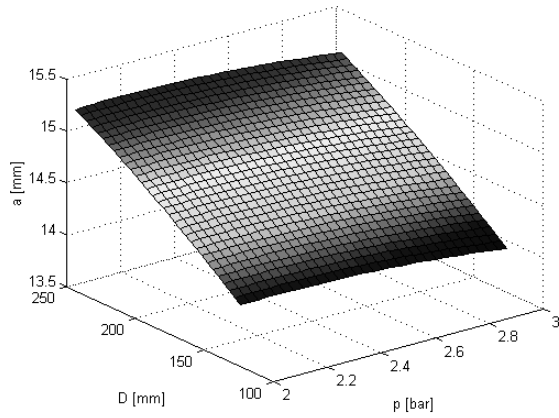
Moreover, from these preliminary results, it seems that the main effect on the parallelepiped dimensions is given by variable  $D$ , i.e., the radial position of the master imprint on the disk. In fact, modifying this value, the resulting variation of the parallelepiped dimension seems to be more than 1mm, while modifying the runner section  $d$ , the parallelepiped dimension changes in the range 0.1 mm – 0.3 mm. An accurate graph analysis shows that the influence of variable  $D$  on parallelepiped dimension  $a$  is approximately linear, since the curvature shown is very small.

When looking for an efficient master location, a good solution would be to place it far from the disk centre and with a large runner section. Moving the attention on how  $\omega$  and  $D$  influence  $a$  (maintaining constant the section  $d$  and pressure  $p$ ), the results show (see Fig.11) that the parallelepiped dimension increases proportionally with both  $D$  and  $\omega$ .

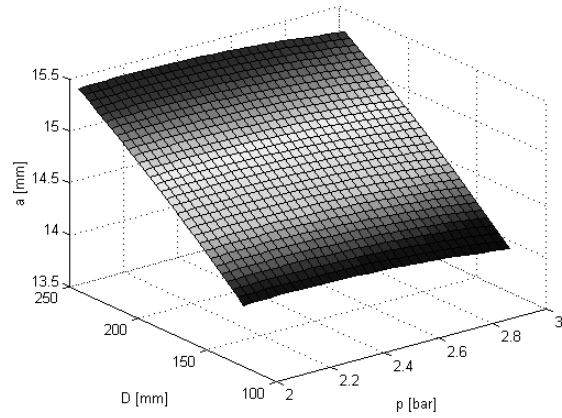


**Figure 11:** a)  $d = 5$  mm and  $p = 2$  bar. b)  $d = 7$  mm and  $p = 2.5$  bar

Also, maintaining constant  $\omega$  and  $d$  and varying  $D$  and  $p$ , the strong influence between  $a$  and  $D$  (see Fig.12) is again evident. It is also possible to see that, increasing  $p$ , the parallelepiped dimension decreases slightly.



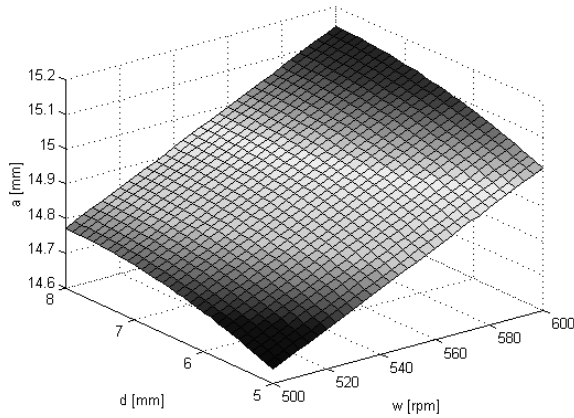
a)



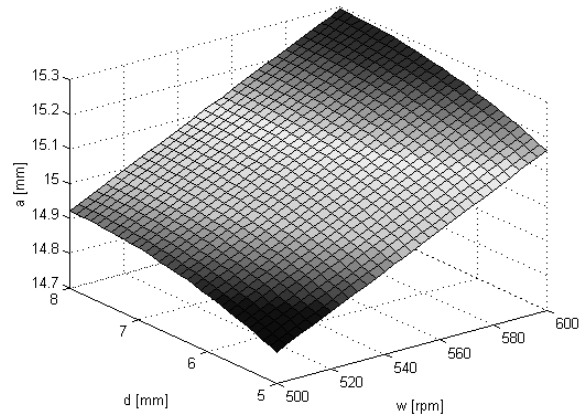
b)

**Figure 12:** a)  $d = 7$  mm and  $\omega = 550$  rpm. b)  $d = 8$  mm and  $\omega = 600$  rpm

Analyzing simultaneously the influence of  $\omega$  and  $d$  on the parallelepiped dimension, the effect of  $\omega$  seems to be stronger than the runner section (see Fig.13).



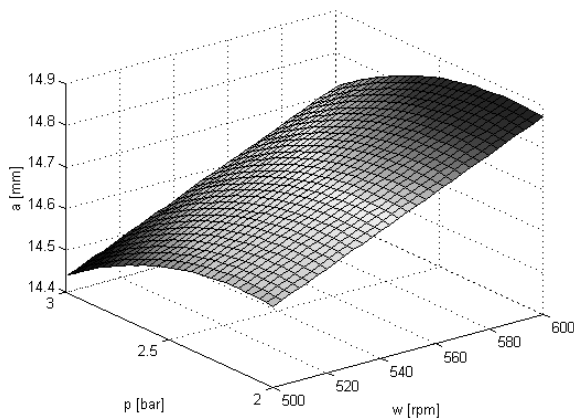
a)



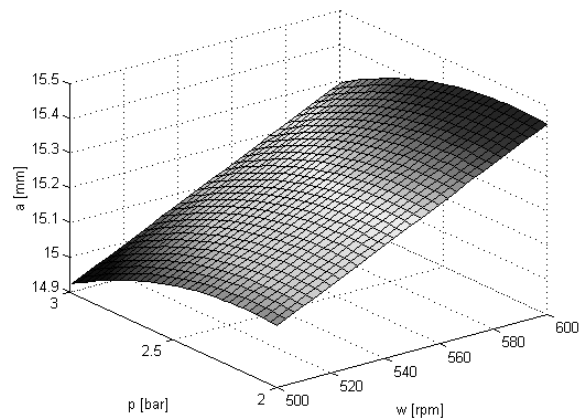
b)

**Figure 13:** a)  $D = 184$  mm and  $p = 2,5$  bar. b)  $D = 244$  mm and  $p = 3$  bar.

Varying  $p$  and  $\omega$  at the same time, it is possible to observe that their influence on the parallelepiped dimension has a non linear behaviour (see Fig.14).



a)



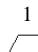
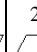
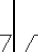
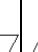

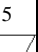
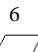
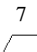
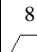
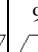

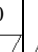
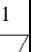
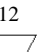
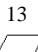
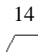
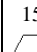
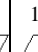
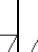
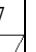
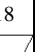
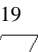
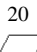
b)

**Figure 14:** a)  $D = 184$  mm and  $d = 6$  mm. b)  $D = 244$  mm and  $d = 8$  mm.

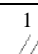
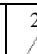
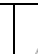


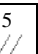
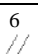


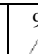

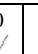
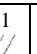
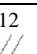
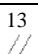

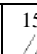
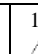
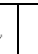
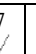
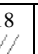
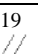
In this case, keeping  $D$  and  $d$  constant, two opposite effects appear: the parallelepiped dimension is inversely proportional to the pressure and directly proportional to the rotational speed. The curvature increase means also that the parallelepiped dimension changes with a quadratic behaviour with both  $p$  and  $\omega$ .

The last evaluation is related to the geometrical tolerances measured on the different cast models (see Tab.8 and Tab.9). These tables show a planarity average value of 0.084 mm with a standard deviation of 0.011 mm, while the parallelism average value between the faces is 0.25 mm with a standard deviation of 0.065 mm.

**Table 8:** Measured planarity error values over the cast parallelepiped (A, ..., M: different masters of a single test; 1, ..., 22: tests with different conditions).

Test n. →	1	2	3	4	5	6	7	8	9	10	11	12	13	14	15	16	17	18	19	20	21	22	
																							
	[mm]	[mm]	[mm]	[mm]	[mm]	[mm]	[mm]	[mm]	[mm]	[mm]	[mm]	[mm]	[mm]	[mm]	[mm]	[mm]	[mm]	[mm]	[mm]	[mm]	[mm]	[mm]	[mm]
<b>A</b>	0.008	0.010	0.012	0.010	0.015	0.002	0.008	0.001	0.004	0.002	0.001	0.002	0.011	0.007	0.009	0.010	0.013	0.014	0.008	0.001	0.009	0.005	
<b>B</b>	0.010	0.003	0.014	0.010	0.015	0.006	0.013	0.003	0.003	0.002	0.004	0.002	0.005	0.002	0.003	0.002	0.002	0.006	0.013	0.004	0.004	0.008	
<b>C</b>	0.009	0.029	0.008	0.009	0.011	0.002	0.004	0.008	0.004	0.003	0.006	0.001	0.006	0.007	0.005	0.011	0.005	0.005	0.004	0.006	0.004	0.004	
<b>D</b>	0.020	0.003	0.003	0.002	0.016	0.002	0.004	0.001	0.003	0.006	0.002	0.009	0.005	0.009	0.009	0.002	0.006	0.011	0.004	0.002	0.004	0.008	
<b>E</b>	0.018	0.011	0.031	0.006	0.001	0.003	0.003	0.002	0.004	0.003	0.000	0.002	0.017	0.002	0.013	0.000	0.006	0.007	0.003	0.000	0.009	0.008	
<b>F</b>	0.020	0.025	0.006	0.002	0.004	0.001	0.002	0.001	0.000	0.002	0.006	0.009	0.004	0.002	0.006	0.005	0.009	0.005	0.002	0.006	0.005	0.007	
<b>G</b>	0.018	0.021	0.032	0.006	0.008	0.000	0.006	0.005	0.002	0.009	0.108	0.013	0.016	0.006	0.007	0.008	0.010	0.008	0.006	0.108	0.016	0.000	
<b>H</b>	0.003	0.003	0.036	0.004	0.012	0.001	0.002	0.004	0.001	0.001	0.003	0.001	0.008	0.009	0.006	0.010	0.001	0.004	0.002	0.003	0.009	0.009	
<b>I</b>	0.022	0.010	0.032	0.006	0.034	0.000	0.003	0.005	0.006	0.004	0.003	0.002	0.010	0.007	0.007	0.002	0.001	0.004	0.003	0.003	0.008	0.006	
<b>L</b>	0.084	0.014	0.001	0.000	0.022	0.004	0.001	0.001	0.008	0.010	0.001	0.008	0.006	0.005	0.008	0.006	0.011	0.004	0.001	0.001	0.006	0.016	
<b>M</b>	0.005	0.002	0.033	0.005	0.019	0.007	0.001	0.003	0.008	0.004	0.001	0.005	0.011	0.006	0.010	0.008	0.005	0.016	0.001	0.001	0.013	0.009	
<b>N</b>	0.057	0.016	0.067	0.005	0.010	0.005	0.013	0.008	0.000	0.003	0.006	0.008	0.005	0.001	0.005	0.005	0.004	0.007	0.013	0.006	0.001	0.007	

**Table 9:** Measured parallelism error values over the cast parallelepiped (A, ..., M: different masters of a single test; 1, ..., 22: tests with different conditions).

Test n. →	1	2	3	4	5	6	7	8	9	10	11	12	13	14	15	16	17	18	19	20	21	22	
																							
	[mm]	[mm]	[mm]	[mm]	[mm]	[mm]	[mm]	[mm]	[mm]	[mm]	[mm]	[mm]	[mm]	[mm]	[mm]	[mm]	[mm]	[mm]	[mm]	[mm]	[mm]	[mm]	[mm]
<b>A</b>	0.185	0.035	0.234	0.241	0.284	0.209	0.210	0.211	0.238	0.241	0.254	0.267	0.271	0.260	0.242	0.265	0.282	0.313	0.316	0.384	0.035	0.282	
<b>B</b>	0.120	0.186	0.240	0.204	0.301	0.205	0.230	0.183	0.185	0.141	0.117	0.154	0.160	0.175	0.224	0.189	0.152	0.111	0.168	0.149	0.186	0.152	
<b>C</b>	0.214	0.484	0.348	0.270	0.360	0.253	0.195	0.214	0.251	0.273	0.236	0.252	0.249	0.237	0.234	0.207	0.270	0.282	0.240	0.347	0.484	0.270	
<b>D</b>	0.233	0.286	0.266	0.193	0.256	0.191	0.170	0.186	0.184	0.235	0.193	0.226	0.250	0.258	0.232	0.247	0.221	0.288	0.277	0.386	0.286	0.221	
<b>E</b>	0.276	0.301	0.448	0.232	0.357	0.230	0.203	0.202	0.237	0.250	0.298	0.256	0.274	0.233	0.247	0.237	0.277	0.317	0.305	0.332	0.301	0.277	
<b>F</b>	0.301	0.347	0.533	0.251	0.330	0.294	0.271	0.282	0.237	0.233	0.271	0.292	0.315	0.290	0.316	0.272	0.343	0.378	0.355	0.356	0.347	0.343	
<b>G</b>	0.347	0.300	0.238	0.208	0.177	0.200	0.193	0.187	0.222	0.215	0.241	0.262	0.256	0.246	0.203	0.250	0.234	0.294	0.285	0.472	0.300	0.234	
<b>H</b>	0.267	0.174	0.377	0.210	0.215	0.213	0.170	0.203	0.222	0.228	0.208	0.244	0.247	0.250	0.230	0.247	0.250	0.294	0.258	0.302	0.174	0.250	
<b>I</b>	0.206	0.301	0.268	0.206	0.318	0.250	0.228	0.226	0.206	0.267	0.254	0.293	0.277	0.275	0.279	0.239	0.301	0.307	0.279	0.277	0.301	0.301	
<b>L</b>	0.264	0.364	0.034	0.206	0.205	0.178	0.215	0.195	0.198	0.226	0.231	0.259	0.267	0.266	0.227	0.252	0.218	0.280	0.254	0.367	0.364	0.218	
<b>M</b>	0.321	0.342	0.364	0.198	0.243	0.228	0.212	0.222	0.256	0.262	0.166	0.247	0.299	0.237	0.262	0.252	0.257	0.299	0.296	0.334	0.342	0.257	
<b>N</b>	0.411	0.395	0.435	0.267	0.315	0.243	0.219	0.202	0.293	0.268	0.223	0.257	0.289	0.262	0.268	0.282	0.254	0.338	0.299	0.333	0.395	0.254	

## 5. Conclusions

Starting from the standard deviation analysis and from the regressive model, it is shown that, in order to obtain a low dimension variation, the most important variable is surely the location of the master with respect to the disk centre. It is in fact evident that, varying this parameter might result in an increased parallelepiped dimensions of more than 1 mm. The position of the imprints on the side of the disk improves the filling process thanks to the presence of a higher centrifugal force entity. The runner diameter is surely less important, even if its role is strongly related to the location of the imprint on the disk. Even though the rotational speed should be kept high, this forces to increase the disk closing pressure, causing, above some values, disk deformation and the consequent deformation of the cast object. From this preliminary experimental approach, it is possible to understand that some more experiments related to the imprints types, shape and volume, should be run in order to investigate their influence on the mould design and process parameters setting. Considering the verified process parameters sensibility, for every casting project it would be very important to perform a preliminary feasibility study in order to reduce the probability of incurring in errors. This could be carried out with the help of simulation tools. At present, there are few commercial tools capable of providing this feature. Nevertheless, it is possible to consider this experimentation as the necessary path to develop a consistent process database for improving the reliability of numerical simulation tools.

## 6. References

1. O. Bjorke, Layer Manufacturing: a Tool for Reduction of Product Lead Time, Trondheim, Norway, 1996.
2. L.J. Barnard, Spin casting as a tool in rapid prototyping, Solid Freeform Fabrication 1999, The University of Texas at Austin, 9-11 August 1999, pp.719-725
3. P.M. Dickens, "Rapid Tooling: A review of the Alternatives", Rapid News, Rapid News publications Ltd., vol.4. n.5,1996,pp.54-62.
4. Z.Huan, G.D. Jordaan, Investigation of the cooling of spin-casting moulds, Applied Thermal Engineering n.23, 2003, pp.17-27
5. Z.Huan, G.D. Jordaan, Galerkin finite element analysis of spin casting cooling process, Applied Thermal Engineering n.24, 2004, pp.95 - 110
6. Z.Huan, G.D. Jordaan, Air-cooling induced from spinning of spin-casting moulds, Applied Thermal Engineering n.25, 2005, pp.1183 - 1194
7. P.M. Hackney, M. Sarwar, S. Widdows, Spin casting of metal parts directly from RP masters, the British Library.
8. Polimeri: proprietà e processi, pubblicazione a cura della Viadelo s.r.l., Milano
9. R. Levi, Elementi di statistica sperimentale, Vico Canavese: Ist. Ric. Tecnologia Meccanica, 1972.
10. G. Vicario, R. Levi, Calcolo delle probabilità e statistica per ingegneri, Eusculapio, Bologna 1998
11. C. Douglas, Montgomery, Controllo statistico della qualità, McGraw-Hill, Milano 2000.